Molecular-dynamics simulation of directional growth of binary mixtures

P. Z. Coura
Departamento de Física, Instituto de Ciências Exatas, Universidade Federal de Juiz de Fora, Juiz de Fora, MG, CEP 36036-330, Brazil

O. N. Mesquita and B. V. Costa
Departamento de Física, ICEx, UFMG, Belo Horizonte, MG, CP 702, 30123-970, Brazil
(Received 17 July 1998)

We use molecular dynamics to simulate the directional growth of binary mixtures. Our results compare very well with analytical and experimental results. This opens up the possibility to probe growth situations which are difficult to reach experimentally, being an important tool for further experimental and theoretical developments in the area of crystal growth. [S0163-1829(99)02405-4]

I. INTRODUCTION

The main aim of this work is to show the feasibility of using molecular-dynamic computer simulations to study directional growth of binary mixtures at atomic level. In computer simulations, we can easily vary parameters of this process and investigate regions of parameter space which are difficult to access experimentally. It is then possible to make predictions that might be useful for basic science or technological purposes.

The rapid expansion of the use of high quality crystalline materials in optical and electronic devices during the past decades has strongly stimulated research, both theoretical and experimental, on dynamics of crystallization. A better understanding about solidification of metals and eutectic fibers are of unquestionable technological interest. Computer simulations have played an important role in the development and understanding of models of crystal growth.[1,2]

During growth, the crystal-fluid interface is not at thermodynamic equilibrium. The moving interface is a dynamical system, which can display a variety of dynamical instabilities and pattern formation. It has become a very important model system for studying complex spatiotemporal dynamics.[3]

A crystal can grow from the adjacent fluid (melt, vapor, or solution) by different mechanisms, depending on the structure of the interface (rough or smooth), material purity, growth rates, temperature gradients, and related factors. For a crystal to grow: (i) atoms or molecules must be transported from the fluid phase towards the interface where the phase transformation is taking place; (ii) transported atoms or molecules must have a nonzero probability of sticking to the crystal surface; (iii) the latent heat generated during crystal growth as well as the excess solute components segregated must be carried away from the interface.

These requirements can be met in a controlled way in experiments of directional growth, where a sample in an appropriate furnace is submitted to a temperature gradient and pulled with a fixed speed towards the colder region of the furnace. For practical crystal growth, the sample can be cast into a quartz tube with chosen diameter and length. This is a three-dimension Bridgman growth arrangement. However, detailed studies about dynamics of crystal growth have been conducted in very thin transparent samples (sandwiched between glass slides), such that the crystal-fluid interface can be visualized and recorded with the use of videomicroscopy techniques.[4,5] Results of such experiments have been compared with results of two-dimensional models of crystal growth. Our computer simulations are also carried out in two dimensions.

As far as we know this is the first attempt to simulate directional growth of a binary mixture utilizing molecular-dynamics (MD) simulation techniques. Some earlier results of MD were reported by Nijemeijer and Landau on laser heated pedestal growth of fibers.[6] Previous simulations consisted of numerical solutions of differential equations for transport of heat and mass, and Monte Carlo techniques to simulate attachment kinetics.[1,2]

With the use of molecular-dynamics techniques we simulate the solidification of a two-component system consisting of solvent (atoms a) and solute (atoms b) interacting via a modified Lennard-Jones (LJ) potential. Particles interact via three different potentials: $\Phi_{a,a}$, $\Phi_{b,b}$, and $\Phi_{a,b}=\Phi_{b,a}$ which we will describe in detail in Sec. III. By tuning the parameters of the LJ potential, we can choose the structure of the interface (rough or smooth) and the segregation coefficient.

In this paper, we simulate a binary system with a rough crystal-fluid interface (like in metals) and with a segregation coefficient of the order of 0.1. The results of these simulations are then compared with well-known models of segregation during directional growth, where diffusion is the only transport mechanism present. This work is organized as follows. In Sec. II we develop the theoretical background on crystal growth of binary mixtures. In Sec. III we discuss the simulation method we have used. In Sec. IV we show our results and discussion, and in Sec. V we present our conclusions.

II. DIRECTIONAL GROWTH OF BINARY MIXTURES

Most models of directional growth are two-dimensional models.[7] Therefore, for comparison with these models, a great deal of experimental observations have been done in thin samples of transparent materials, where presumably the

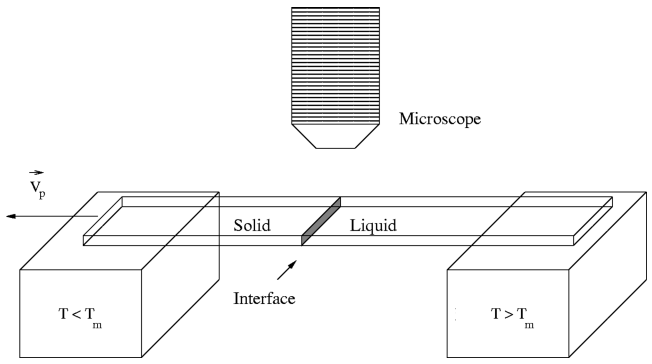

FIG. 1. Basic experimental setup for directional growth (as described in the text). The interface motion can be visualized using an optical microscope. T_m is the melting temperature of the mixture.

third dimension is not important, and the crystal-fluid interface can be followed in time, by using videomicroscopy with digital image analysis.[4,5] The usual experimental setup is shown in Fig. 1. The furnace consists of two metal blocks at controlled temperatures: one block with temperature above the sample melting temperature and the other below. A thin sample of the material to be studied is sandwiched between glass slides with spacers, whose thickness is in general of a few micra, to keep the system as close as possible to a $2d$ geometry, and guarantee that the transport of mass is mainly diffusive with no convection in the fluid phase. The sample is then put on top of the metal blocks, with good thermal contact. A temperature gradient appears along the sample cell. The sample is then pulled towards the colder block in a very precise and controlled way by a pulling system and starts to solidify. After an initial transient the system achieves a steady state where the interface position becomes fixed in the laboratory frame, the growth speed is the same, but opposite to, the pulling speed, and the solute concentration profile becomes steady in the laboratory frame.

An example of solute segregation during directional solidification of binary mixture composed by the crystal caprolactane as solvent and methyl-blue as solute[8] is observed with videomicroscopy (Fig. 2). In the top part of Fig. 2 we show an image of the crystal (left side) and melt (right side), with maximum concentration of methyl-blue at the melt side of the interface. From the gray level of the image we obtain the methyl-blue concentration profile across the sample, which, in the melt, decays exponentially as a function of the distance from the interface (bottom part of Fig. 2). We will see that molecular-dynamics simulations can reproduce very well this type of result.

Morphological instabilities of the planar interface are inhibited during directional growth of pure materials. However, for binary systems, depending on concentration of solute, temperature gradient, and growth speed, morphological instabilities can occur, the planar interface becoming cellular and eventually dendritic. This is the Mullins-Sekerka instability.[9] In our simulations we are able to observe both regimes: planar and cellular interfaces. In this work we will focus our attention on the evolution of a planar interface, where we clearly see segregation and transport of solute at the interface. From the data analysis we obtain the solute concentration profile, the segregation coefficient for this binary system, and the diffusion coefficient of the solute in the solvent.

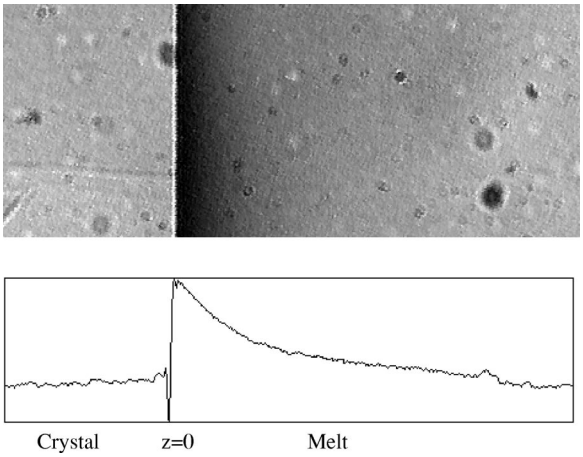

FIG. 2. Directional solidification of the binary mixture caprolactane (solvent) and methyl-blue (solute). Liquid is at the right side and solid to the left side. Methyl-blue concentration is proportional to the gray level of the image. The lower plot shows the methyl-blue concentration as a function of position.

A. Binary phase diagram

An added second component (solute) in a crystal-fluid system (solvent) is, in general, more soluble in the fluid phase than in the solid phase, since the mismatch in size and shape between solvent and solute atoms may cause a large mechanical (geometrical) stress in the crystalline lattice of the solid phase. In this case the segregation coefficient K which is the ratio between the solute concentration in the solid (c_S) and the solute concentration in the liquid (c_L), satisfies $K=c_S/c_L<1$. In our simulations we observed that the value of the segregation coefficient is very sensitive to the σ_{ab} parameter of the LJ potential, that controls the effective size difference between solvent and solute atoms, and less sensitive to changes in the depth of the potentials. The stress in the crystalline lattice increases with increasing σ_{ab} and consequently a large σ_{ab} reduces K.

For diluted binary systems a sketch of a phase diagram for $K<1$ is shown in Fig. 3. The melting temperature of the mixture decreases with increasing solute concentration. The

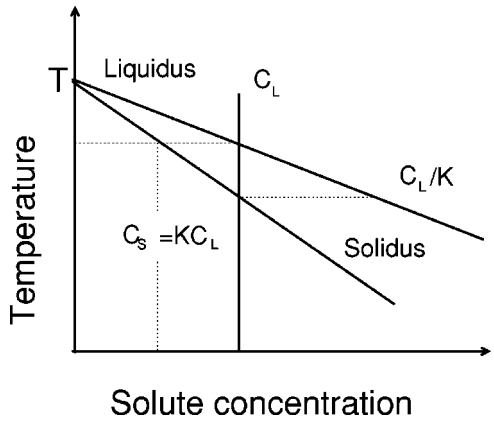

FIG. 3. Schematic drawing of part of binary system phase diagram, the solute has $K<1$.

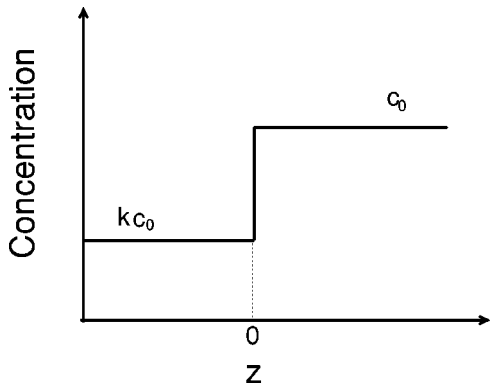

FIG. 4. Solute concentration profile near an equilibrium solid-liquid interface, for a solute concentration in the melt equal to c_0 and $K<1$.

liquidus and solidus lines define the temperature as a function of solute concentration where the first solid is formed and where the sample is completely solidified, respectively. If we name the slopes of the liquidus and solidus lines by m and m', respectively, the segregation coefficient K can also be written as $K=m/m'$.[2]

In Fig. 4 we show the solute concentration profile for an equilibrium crystal-fluid interface where the solute concentration in the liquid is c_0 and consequently the solute concentration in the solid is $c_S=Kc_0$. Usually, this is the initial condition for most directional growth experiments. Since in the present work we will be more interested in the steady-state situation (Fig. 5), the initial condition is not important.

B. Solute transport

Since our system is two-dimensional, if we consider a planar interface along x and growth direction along z, for large systems and far from the edges of the sample cell, the solute concentration profile will be a function of only the time variable t and the space variable z. It is convenient to write the transport equations in the system of reference of the moving interface, since in this frame of reference it is possible to have a steady-state situation, where the solid growth velocity (V_s) is equal and opposite to the pulling velocity (V_p) and the solute concentration profile is constant in time. The steady-state situation is achieved when the segregated-solute-flux at the interface is equal to the solute-flux away from the interface, in the fluid phase. In general, for solid-liquid interfaces the difference in density between the solid and liquid phases is negligible. Due to mass conservation, the average growth velocity of the solid phase (V_s) is equal to the average velocity of decrease of the fluid phase (V_f). However, if the fluid phase is less dense than the solid phase, again for mass conservation, $J_s=\rho_s\times V_s$ and $J_f=\rho_f\times V_f$ and since $J_s=J_f$, then $V_f=V_s\times\rho_s/\rho_f$, where J_s,ρ_s and J_f,ρ_f are the mass flux and density in the solid and fluid phases, respectively. At steady state $V_s=V_p$ so that

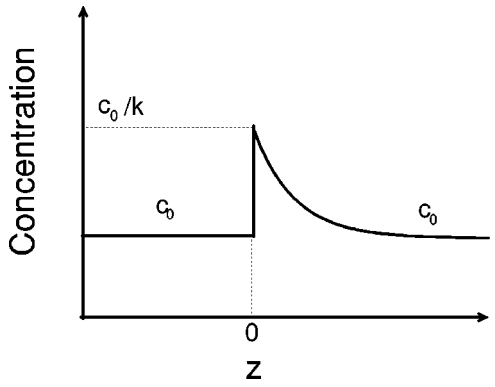

FIG. 5. Solute concentration profile near a steady-state advancing solid-liquid interface for $K<1$.

$$V_f=V_p\times\rho_s/\rho_f. \tag{1}$$

Since the solute diffusion coefficient in the solid phase is orders of magnitude smaller than the one in the fluid phase, the transport of solute in the solid phase can be neglected. Therefore, we will consider only the solute transport in the fluid phase. In the moving crystal-surface reference frame (system of reference moving with velocity V_s) the diffusion equation for the solute concentration in the fluid phase (c_f) can be written as:[7]

$$\frac{\partial c_f}{\partial t}=D\frac{\partial^2 c_f}{\partial z^2}+V_f\frac{\partial c_f}{\partial z}, \tag{2}$$

where D is the solute diffusion coefficient in the fluid phase and V_s and V_f where defined above. Equation (2) must be supplemented with boundary conditions: (a) $c_f=c_0$ at $z=$infinity, (b) $(1-K)V_f c_f=-Ddc_f/dz$ at $z=0$. The condition (b) is just the solute mass conservation at the interface.

At steady state V_s and V_f are constant and $V_s=V_p$. The solution of the above equation is:

$$\begin{aligned} c_L(z)&=c_0\left[1-\left(\frac{1-K}{K}\right)\exp\left(-\frac{V_f z}{D}\right)\right]\\ &=c_0\left[1-\left(\frac{1-K}{K}\right)\exp\left(-\frac{V_p\rho_s z}{\rho_f D}\right)\right], \end{aligned} \tag{3}$$

where in the last equality we used Eq. (1). At steady state, the solute concentration in the solid is constant and equal to c_0. In Fig. 5 we show the theoretical prediction for the solute concentration profile during steady-state directional growth. This is the experimentally observed behavior as shown in Fig. 2. Our molecular-dynamics results for solute segregation during directional growth display the same type of behavior as will be shown in Sec. IV. An important length scale for this problem is the diffusive length $l_D=D\rho_f/V_p\rho_s$. The system can be considered large for boundary condition (a) to apply, if the length of the fluid phase along z is much larger than l_D.

III. SIMULATION

Our simulation is carried out using molecular-dynamics approach with all particles interacting through a modified LJ potential.

$$\Phi_{i,j}(r_{i,j})=\begin{cases}\phi_{i,j}(r_{i,j})-\phi_{i,j}(r_c)-\left(\dfrac{d\phi_{i,j}(r_{i,j})}{dr_{i,j}}\right)_{r_{i,j}=r_c}(r_{i,j}-r_c) & r_{i,j}<r_c\\ 0 & r_{i,j}>r_c,\end{cases}$$

where $\phi_{i,j}(r_{i,j})$ is the LJ(12-6) potential:

$$\phi_{i,j}(r_{i,j})=\epsilon_{i,j}\left[\left(\frac{\sigma_{i,j}}{r_{i,j}}\right)^{12}-\left(\frac{\sigma_{i,j}}{r_{i,j}}\right)^{6}\right]. \tag{4}$$

The indexes i and j stand for particles in the positions $\mathbf{r}_i$ and $\mathbf{r}_j$, respectively, and $0\leqslant i,j\leqslant N$, where N is the total number of particles and $r_{i,j}=|\mathbf{r}_i-\mathbf{r}_j|$. A cutoff $r_c=2.5\sigma_{aa}$ is introduced in the potential in order to accelerate the simulation. If the force on a particle is found by summing contributions from all particles acting upon it, then this truncation limits the computational effort to an amount proportional to the total number of particles N. Of course this truncation introduces discontinuities both in the potential and force. To smooth this discontinuity we introduce the constant term $\phi(r_c)$. Another term $(d\phi/dr)_{r=r_c}(r-r_c)$ is introduced to remove the force discontinuity. Particles in our simulation move according to Newton's law, that generate a set of $2N$ coupled equations of motion which are solved by increasing forward in time the physical state of the system in small time steps of size $\Delta t=0.02\sigma_{aa}(m_a/\epsilon_{aa})^{1/2}$. The resulting equations are solved by using Beeman's method of integration. In order to improve the method we use a Verlet and a cellular table.[10] The Verlet table consists of an address vector which contains the number and position of each particle inside a circle of radius $r_v=3\sigma_{aa}$. After some steps in time, the neighborhood of each particle changes, so that we have to refresh the Verlet table. This refreshment process can take a long time. In order to make it shorter we divide the system in cells of size $c_x\times c_z=(3.5\sigma_{aa})^2$, such that in recalculating the Verlet table we have to search only in neighbor cells.

Initially we distribute $N=n_x\times n_z=27\times 270$ particles over the two-dimensional surface $L_x\times L_z=27\times 2^{1/6}\times 451\sigma_{aa}^2$. We assume periodic boundary conditions in the x direction. In the z direction we divide the system in two distinct regions, a solid and a fluid one. In the solid region particles stand initially in their equilibrium position in a total of 27 $\times 30$ particles. On the fluid region the density is initially $\rho=0.5\sigma_{aa}^{-2}$, giving a total of 27×240 particles, randomly distributed in a triangular lattice and slightly dislocated from their equilibrium position. We impose a temperature gradient along the z direction using a velocity renormalization approach.[10] We divide the system in two regions: The first one defined by $-210\sigma_{aa}\leqslant z\leqslant -231\sigma_{aa}$, where temperature is fixed to $T_0=0$, the other one defined by $80\sigma_{aa}\leqslant z\leqslant 220\sigma_{aa}$, where the temperature is fixed to T_h, higher than the melting temperature T_m of the pure material. We let the system evolve for 1.2×10^5 steps in time of size Δt, which seems to be enough to equilibrate the system. Once the equilibrium is reached we start pulling the system in the $-z$ direction, at a pulling velocity $v_p=4\times 10^{-3}(\epsilon_{aa}/m_{aa})^{1/2}$. Particles which reach z_{min} are frozen, working as a sink. Once a bunch of particles are frozen at z_{min} the same amount is introduced at z_{max} with the same solute initial concentration.

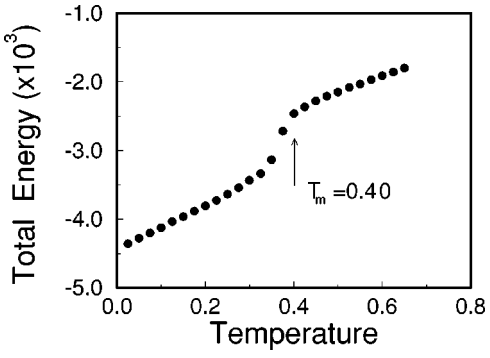

FIG. 6. Plot of total energy as function of temperature for the pure material.

In order to obtain an estimate for T_m we did an independent simulation with 1.5×10^3 particles in a box of fixed dimensions and initial density $0.5\sigma_{aa}^{-2}$, below the solid density. The result is shown in Fig. 6. We can see that $T_m=0.40\times\epsilon_{aa}/k_B$.

A. Units

In our simulation we consider a system consisting of two different types of particles: the solvent (a particles) and the solute (b particles). We define three types of interactions, solute-solute (b-b), solvent-solvent (a-a), and solute-solvent (b-a). The initial solute concentration is $c_0=5\%$. This concentration is defined as the ratio between the number of particles of the solute and the total number of particles of the solvent. To calculate the density along the crystal being grown we use strips of size $\Delta z=20\sigma_{aa}$ (so that we can easily map the impurity concentration along the crystal). As a matter of simplicity, from now on we measure energy in units of ϵ_{aa}, distance in units of σ_{aa} and mass in units of m_a, and we chose the LJ parameters as $\epsilon_{ab}=0.5$, $\epsilon_{bb}=0.1$, $\sigma_{ab}=\sigma_{bb}=\sigma_{aa}=1$, and $m_b=m_a=1$. Also, we measure temperature and time in units of ϵ_{aa}/k_B and $(m_a\sigma_{aa}^2/\epsilon_{aa})^{1/2}$, respectively.

IV. RESULTS

We observed a decrease in computation time to achieve steady state as the density of the fluid was decreased. Therefore we worked with a fluid density 5.7 times smaller than the solid density, as can be seen from the density profile shown in Fig. 7. For a given pulling speed V_p the time for the system to achieve steady state, and consequently the simulation time, is of the order of $\sim D/V_f^2=D/V_p^2(\rho_s/\rho_f)^2$. Since D in the fluid phase increases with decreasing ρ_f/ρ_s, but not as fast as $(\rho_f/\rho_s)^2$, by decreasing the fluid density

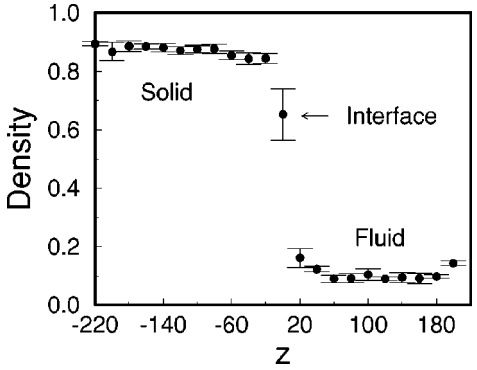

FIG. 7. Density profile in our simulation. The solid phase density was 5.7 times larger than the fluid phase density.

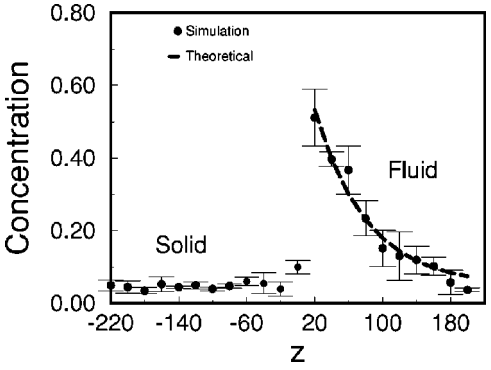

FIG. 9. Plot of the fraction of solute along the crystal. The interface is at $z \approx 0$. Solute segregation at the interface is clearly seen.

the computation time δt also decreases.

For $\rho_{f1}=0.7$ (liquid) and $\rho_{f2}=0.15$ (vapor) we obtained, respectively, $D_1 \approx 0.1$ and $D_2 \approx 1.2$. Therefore $\delta t_2/\delta t_1 \sim D_2(\rho_{f2})^2/D_1(\rho_{f1})^2 \sim 0.55$, since ρ_s and V_p are constants, the computation time decreased by almost a factor of 2 as the fluid density decreased by almost a factor of 6. As far as diffusive transport is assured the large density difference between the two phases will not change, either qualitatively or quantitatively, the conclusions drawn from Sec. II B. Computer efficiency can be improved by increasing the mass ratio. We, however, did not make systematic simulations with different mass ratios, since we had already a large number of parameters to vary.

We checked the velocity profile of the fluid phase and determined that the solute transport is mainly diffusive for our simulations. Therefore the solute concentration profile should follow the behavior predicted by Eq. (3).

A. Interface structure for pure material

It is the structure of the interface at atomic level that determines if a particular crystal will display faceted (smooth interface) or nonfaceted (rough interface) morphology. Fluid particles will attach preferably on kink sites on the interface. On smooth interfaces, kink sites are created by two-dimensional nucleation or by screw dislocations through growth steps. Lateral growth (layer-by-layer) occurs by attachment of fluid particles at growth steps. On the other hand, on rough interfaces, thermodynamic fluctuations can create many kink sites. The fluid particles then attach to those sites and growth proceeds normally to the interface, because no lateral displacement of growth steps is required.

A criterion to determine if a particular solid-fluid interface will be smooth or rough at atomic level was introduced by K. A. Jackson.[2] Modeling the solid-fluid interface as an Ising system, he introduced the α factor defined as $\alpha=\xi L/k_b T_m$, where L is the latent heat of the transformation per particle, T_m is the temperature of the transformation, k_B the Boltzmann constant, and ξ is the ratio between the number of nearest neighbors at the interface and the number of nearest neighbors in the bulk. If $\alpha > 2$ the interface is smooth, if $\alpha < 2$ the interface is rough. Even though this is a semiquantitative criterion it works very well for solid-liquid transformations. Metals growing from the melt usually have $\alpha < 1$ and do not present facets. With this criterion transparent materials which solidify like metals were discovered. They are the so-called plastic crystals with α factors smaller than 1. From the data of energy as a function of temperature for the pure system displayed in Fig. 6 one can obtain the latent heat of the transformation $L=0.59$ and the melting temperature $T_m=0.40$. For a two-dimensional triangular lattice and direction of growth (0,1), $\xi=2/3$. Since we are using $k_B=1$ we obtain $\alpha=0.98$, a typical value for metals. Indeed, the interface displays a morphology of rough interface and no evidence of faceting was found.

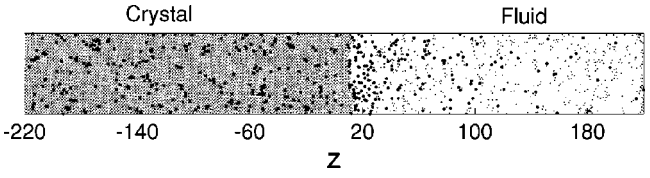

FIG. 8. Typical result for the crystal growth simulation using the parameters set described in the text. Larger circles represent solute and smaller represent solvent. A higher solute concentration is clearly observed near the fluid side of the interface.

B. Solute concentration profile

Our simulations of directional growth were done with solute concentration in the fluid of $c_0=5\%$, for fixed pulling velocity of $V_p=0.004$. An example of solute segregation by the crystal-fluid interface during growth is shown in Fig. 8.

After averaging over many runs to improve statistics one obtains the steady-state solute concentration profile represented as data points with error bars in Fig. 9 (compare this with Fig. 2).

A fit of the concentration profile in the liquid using Eq. (3) is displayed as a dashed curve. From this fit one obtains $K=0.094\pm0.005$ and an effective diffusion length $l_D=60\pm5$. Using Eq. (3), with $\rho_s/\rho_f=5.7$ and $V_p=0.004$, we obtain an effective diffusion constant $D=1.4\pm0.1$. To measure D independently we use the relation $\langle r^2\rangle=4Dt$, where r is the displacement of b particles and t is time. We obtain an effective diffusion constant $D=1.3\pm0.1$. By calculating D from the velocity-velocity correlation function we obtain essentially the same result. Therefore, quantitative results can be obtained from molecular-dynamics simulation of directional growth of binary mixtures.

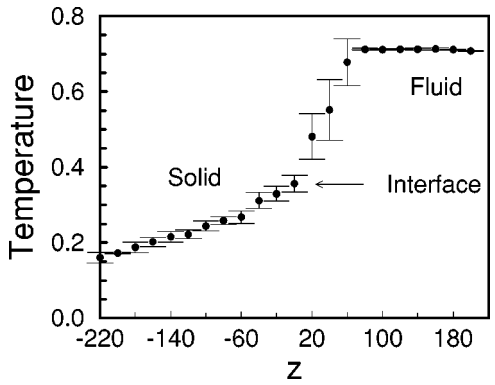

FIG. 10. Temperature profile across the sample. At $z<-220$ the temperature is fixed at $T=0$ and between $80\leqslant z\leqslant 220$ is fixed at $T=0.70$.

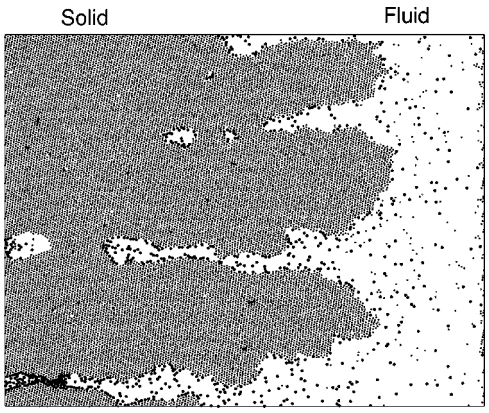

FIG. 11. Example of cellular instability originated after K was decreased by tuning $\sigma_{a,b}$ of the LJ potential. Larger circles represent solute and smaller represent solvent particles.

C. Thermal length and cellular instability

The temperature profile inside the material is shown in Fig. 10. We see that the first solid formed is at temperature of ~ 0.35. The melting temperature of the pure material is 0.40. Therefore $mC_0 \sim 0.40-0.35=0.05$. Since the thermal length $l_T=mc_0(1-K)/KG$,[7] $K\approx 0.1$, and $G\approx 0.005$ we obtain the value $l_T\sim 20$. Because $l_D \gg l_T$ we are in the stable region for a cellular instability, i.e., the interface remains planar. By decreasing K and increasing V_p we can make $l_T > l_D$ and observe a cellular instability as seen in Fig. 11. A detailed study of cellular instabilities using molecular-dynamics simulations is under way and will be the subject of a future publication.

V. CONCLUSIONS

By using molecular dynamics we simulated the directional growth of binary mixtures in a LJ system. Our simulations are able to generate segregation profiles similar to the ones observed experimentally. Comparison with analytical results from literature shows that our simulations give quite good quantitative results. The great advantage of simulations is that we can access a wide region of interesting parameters by simply tuning the LJ potential. It is then possible to easily investigate regions that are difficult to access experimentally.

ACKNOWLEDGMENTS

This work was partially supported by FAPEMIG, CNPq, and CAPES. Numerical calculations were done at the CENAPAD and in the Pentium cluster at the Laboratório de Simulação, Departamento de Física, ICEx, UFMG.

[1] J. D. Weeks and G. H. Gilmer, Adv. Chem. Phys. **40**, 157 (1979).
[2] D. P. Woodruff, *The Solid-Liquid Interface* (Cambridge University Press, London, 1973).
[3] M. C. Cross and P. C. Hohenberg, Rev. Mod. Phys. **65**, 851 (1993).
[4] J. D. Hunt, K. A. Jackson, and H. Brown, Rev. Sci. Instrum. **37**, 805 (1966).
[5] J. M. A. Figueiredo, M. B. L. Santos, L. O. Ladeira, and O. N. Mesquita, Phys. Rev. Lett. **71**, 4397 (1993).
[6] M. J. P. Nijmeijer and D. P. Landau, Comput. Mater. Sci. **1**, 389 (1993).
[7] J. S. Langer, Rev. Mod. Phys. **52**, 1 (1980).
[8] U. A. Batista and O. N. Mesquita (unpublished).
[9] W. W. Mullins and R. F. Sekerka, J. Appl. Phys. **34**, 323 (1963); **35**, 444 (1964).
[10] M. P. Allen and D. J. Tildesley, *Computer Simulation of Liquids* (Oxford Science Publications, New York, 1992).